<Original>

Stress Intensity Factors for Branched Edge Cracks

Inhoy Gu*

(Received August 30, 1985)

가지친 표면크랙의 응력확대계수

구　　인　　회

초　　록

무한평판에 묻혀진 크랙에 대한 응력확대계수를 결정하는 전위분포법을 반무한 평판에서의 표면 크랙에 확장 적용하였다. 이를 위해 반평면에서의 전위응력의 기본 해가 간단한 복소수 응력함수형 태로 얻어졌다. 평형을 이루는 절편적인 분포로부터 응력확대의 계수를 계산하는 새로운 방식을 제 안하였으며 수직표면 크랙과 묻혀진 경사크랙에 대한 기존해와 이 방법의 결과가 상호 비교되었다. 경사진 표면크랙에 대한 계산결과는 유한평판에서의 기존하는 Mapping Collocation 해석과 비교되 어 좋은 일치를 보여 주었다. 구부러진 크랙과 대칭으로 가지친 크랙에 대해서는 표면크랙과 묻혀진 크랙사이에 상당한 차이가 있음이 나타났다.

1. Introduction

The present paper is concerned with oblique edge and branched edge cracks in a semi-infinite plane of brittle homogeneous isotropic material. A primary interest in the linear elastic fracture mechanics including small-scale yielding fracture is in the stress distribution near a crack tip, namely the stress intensity factor

and its related properties, which are considered to be well established in this field.

Practical significance in dealing with edge cracks arises in many situations. Fatigue cracks are initiated from the free surface. And many cracks found in service conditions are either bent or branched. Since fracture from microstructural observations can be classified in general into the shear and opening mode fracture, the transition between the two modes may comprise the angle change of a crack path, i.e., a bent crack. Environmentally induced cracks such as various corrosion cracks must be edge cracks,

* Member, Dept. of Mechanical Engineering, Chung Ang University

which usually become branched under tension.

Extensive studies have been carried out for the bent and branched cracks embedded in an infinite plane, as well surveyed in Lo[1] and Cottrell and Rice[2]. It seems often assumed that an embedded crack symmetrical about a loading axis is an approximation for a crack emanating from a free surface[3]. The present analysis shows a substantial difference between the two cases, and a simple correction factor appears to have a limited validity.

There are many methods—analytical and numerical—for determining the stress intensity factors. Among them one of powerful methods seems to be the assumption of dislocation arrays along a crack-line. Instead of the continuous distribution of dislocations, we use the method of discrete dislocations, which was developed by Vitek[3] for the problem of branched cracks embedded in an infinite plane. Advantages in using the method are; it is simple and straightforward in usage, for no singular integral equations are involved. The Green's functions in the boundary integral method are not readily available for complex crack shapes. One of the powerful points in the discrete dislocation method is that it has no restrictions on the crack shapes, as will be seen later. A new computational scheme for accurate stress intensity factors is attempted from the equilibrium Burger's vectors near a crack tip. Applications of the method to the problems with exact solutions such as a normal edge crack and an embedded angled crack show that highly accurate results can be obtained with linear algebraic equations of around 100 unknowns about the magnitudes of of Burger's vector of discrete dislocations.

2. Dislocation Model for Cracks in Half-Plane

A crack-line in a half-plane is replaced by an array of discrete edge dislocations with slip planes normal and parallel to the crack-line. The dislocations are distributed to have equilibrium stresses with applied stresses so that the crack face can be traction-free. For the purpose of calculating dislocational stresses, we first derive the stress functions of an isolated dislocation in an isotropic semi-infinite plane.

The elastic stress components in plane elasticity problems are expressed in terms of the complex potential functions $\phi(z)$ and $\psi(z)$ of the complex variable $z=x+iy$[4].

$$\sigma_x+\sigma_y=2[\phi'(z)+\overline{\phi'(z)}]$$
$$\sigma_y-\sigma_x+2i\tau_{xy}=2[\bar{z}\phi''(z)+\psi'(z)] \qquad (1)$$

where the superposed bar denotes the complex conjugate, and $\phi'(z)=\dfrac{d}{dz}\phi(z)$, $\phi''(z)=\dfrac{d^2}{dz^2}\phi(z)$. When an edge dislocation with Burger's vector $\boldsymbol{b}=(b_x,b_y)$ is located at $z_0=x_0+iy_0$ in an infinite isotropic elastic plane, the complex potential functions are

$$\phi_0(z)=\gamma\ln(z-z_0)$$
$$\psi_0(z)=\gamma\ln(z-z_0)-\gamma\bar{z}_0/(z-z_0) \qquad (2)$$

where $\gamma=\dfrac{G(b_y-ib_x)}{4\pi(1-\nu)}$ \qquad (3)

in a plane strain condition, and G is the shear modulus and ν is Poisson's ratio. For a dislocation near an elliptical hole, as shown in Fig. 1, there has to be an image stress field for the traction-free condition on the hole surface. Employing the conformal mapping technique, we transform the ellipse in the z-plane into a circle of unit radius in the ζ-plane. Thus the region is defined for $|\zeta|>1$.

$$z=R(\zeta+m/\zeta) \qquad (4)$$

where $R=(a+b)/2$, $m=(a-b)/(a+b)$. The complex potentials for the image stress field were obtained by Vitek[5] using the Cauchy integral method.

$$\phi_1(\zeta)=2\gamma\ln\zeta-\gamma\ln(\zeta-m/\zeta_0)$$
$$-\gamma\ln(\zeta-1/\bar{\zeta}_0)+\frac{\bar{\gamma}}{\zeta_0\bar{\zeta}_0(\bar{\zeta}_0{}^2-m)}[\zeta_0(1+m\bar{\zeta}_0{}^2)$$

$$-\bar{\zeta}_0(\zeta_0{}^2+m)]\frac{1}{\zeta-1/\bar{\zeta}_0} \qquad (5)$$

$$\psi_1(\zeta)=2\bar{r}\ln\zeta-\bar{r}\ln(\zeta-m/\zeta_0)-\bar{r}\ln(\zeta-1/\bar{\zeta}_0)$$

$$+\frac{r}{\zeta_0\bar{\zeta}_0(\zeta_0{}^2-m)}[\bar{\zeta}_0(\zeta_0{}^2+m^3)$$

$$-m\zeta_0(\bar{\zeta}_0{}^2+m)]\frac{1}{\zeta-m/\zeta_0}$$

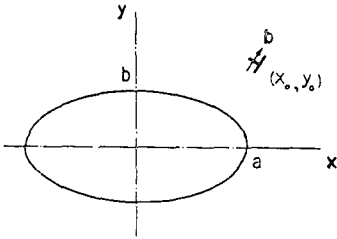$$-\zeta\frac{1+m\zeta^2}{\zeta^2-m}\phi_1{}'(\zeta) \qquad (6)$$

Fig. 1 An edge dislocation near an elliptical hole

where ζ_0 is the transformation of z_0 from the equation (4). These complex potentials can be further transformed to be appropriate to our problem in the half plane defined for $x>0$. Consider a limiting case of the ellipse by letting the semi-axis a of the ellipse go to zero. Then the equation (4) can be written as

$$\zeta=\left(\frac{z}{b}\right)+\sqrt{\left(\frac{z}{b}\right)^2+1}$$

Using the condition $z/b\ll1$ of the semi-infiniteness, we get

$$\zeta=\left(\frac{z}{b}\right)+1$$

$$\frac{1}{\zeta}=-\left(\frac{z}{b}\right)+1 \qquad (7)$$

Substituting the equation (7) and the corresponding transformation of z_0 into the functions (5) and (6), and from the semi-infinite plane condition, one can obtain a compact form of the functions after routine mathematical manipulations.

$$\zeta_1{}'(z)=-\frac{r}{z+\bar{z}_0}+\frac{\bar{r}(z_0+\bar{z}_0)}{(z+\bar{z}_0)^2} \qquad (8)$$

$$\phi_1{}'(z)=-\frac{r+\bar{r}}{z+\bar{z}_0}+\frac{\bar{r}(z_0+\bar{z}_0)+rz}{(z+\bar{z}_0)^2}$$

$$-\frac{2\bar{r}z(z_0+\bar{z}_0)}{(z+\bar{z}_0)^3} \qquad (9)$$

In a similar way, when the surface $y=0$ is a free surface with a region defined for $y<0$, we let $b\to0$ and $z/a\ll1$. Then the stress functions for the dislocational image stresses are given as follows for the half plane $y<0$.

$$\zeta_1{}'(z)=-\frac{r}{z-\bar{z}_0}-\frac{\bar{r}(z_0-\bar{z}_0)}{(z-\bar{z}_0)^2} \qquad (10)$$

$$\phi_1{}'(z)=\frac{r-\bar{r}}{z-\bar{z}_0}+\frac{\bar{r}(z_0-\bar{z}_0)-rz}{(z-\bar{Y}_0)^2}$$

$$-\frac{2\bar{r}z(z_0-\bar{z}_0)}{(z-\bar{z}_0)^3} \qquad (11)$$

Complete stress distress distributions around an edge dislocation in the semi-infinite plane are calculated from the equation (1) with the superposed potential functions.

$$\phi'(z)=\phi_0{}'(z)+\phi_1{}'(z)$$

$$\psi'(z)=\psi_0{}'(z)+\psi_1{}'(z) \qquad (12)$$

The above solution yields an identical result to Hirth and Lothe[6] in a particular case of $b=(1,0)$.

As mentioned earlier, discrete dislocations are distributed along a crack-line of length l in a continuous half plane subject to a remotely applied tension, as illustratee in Fig. 2. First we divide the crack-line into n segments, and at the ith dividing point z_{0i}, two dislocations are located with Burger's vectors of magnitudes $b_{i,1}$ and $b_{i,2}$, normal and parallel to the crack-line respectively. Note that z_{0n} is the crack tip point $(s=l)$ of a stress singularity. Due to the presence of the dislocations, tractions along the crack-line should be vanished. With respect to the center of each segment $z_j=(z_{0j-1}+z_{0j})/2$, the notations $\sigma_n(z_j,z_{0i})$ and $\tau_s(z_j,z_{0i})$ are given to the normal and shear stresses at z_j due to the dislocation of unit vector at z_{0i}, and $\sigma_n(z_j)$ and $\tau_s(z_j)$ denote the applied stress components at z_j in the uncracked plane. Thus the equations to determine $2n$ unknown b_i's can be written as follows.

$$\sum_{i=1}^{n} [b_{i,1}\sigma_{n,1}(z_j, z_{0i}) + b_{i,2}\sigma_{n,2}(z_j, z_{0i})]$$

$$+ \sigma_n(z_j) = 0$$

$$\sum_{i=1}^{n} [b_{i,1}\tau_{s,1}(z_j, z_{0i}) + b_{i,2}\tau_{s,2}(z_j, z_{0i})]$$

$$+ \tau_s(z_j) = 0 \tag{13}$$

where the subscript 1, 2 corresponds to the Burger's vector normal and parallel to the crack-line respectively.

In the model of a continuous distribution of dislocations with a density $B(s)$, the stress intensity factor k can be determined from the Burger's vector near the crack tip ($s \rightarrow l$ in Fig. 2)[7].
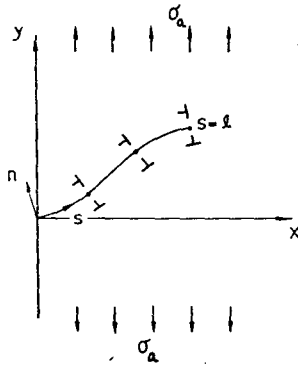

Fig. 2 Dislocational model of a crack-line in the half-plane

$$\int B(s)ds = \frac{2(1-\nu)k}{G\sqrt{2\pi}} \int \frac{ds}{\sqrt{l-s}} \tag{14}$$

where the mode I and II stress intensity factors are $k = k_1{}^*$ and $k = k_{II}$ for the Burger's vector normal $(b_{i,1})$ and parallel $(b_{i,2})$ to the crack-line respectively. In the present analysis, as a discrete dislocation is located at the right hand side of each segment, a special computational scheme is developed for accurate stress intensity factors. Taking the last two segments near the crack tip, one can get from the equ-

* The stress intensity factor is defined as in

$$\sigma_{ij} = \frac{k_1}{\sqrt{2\pi r}} f_{ij}(\theta) + O(\sqrt{r})$$

ation (14)

$$k_l = \frac{b_n + b_{n-1}}{\sqrt{2}} \frac{G\sqrt{2\pi}}{4(1-\nu)\sqrt{\Delta l}} \tag{15}$$

where Δl is an interval in the equal division of the crack-line. This expression was found to provide a slightly lower value when applied to the problems of a normal edge crack in a half plane and an embedded angled crack. In a similar fashion, with respect to the second division $(i = n-1)$ from the crack tip, the equation (14) gives another expression, which was a slight upper bound.

$$k_u = \frac{b_{n-1}}{\sqrt{2}-1} \frac{G\sqrt{2\pi}}{4(1-\nu)\sqrt{\Delta l}} \tag{16}$$

Thus the mean value of the above two expressions is expected to be an accurate solution, relatively irrespective of the number of divisions

$$k = (k_l + k_u)/2 \tag{17}$$

This computational scheme was tested upon the problem of an angled crack embedded in an infinite plane under uniform tension, for which the image stresses are non-existant. With a total number of 100 unknowns, the equation (17) gave an error less than 1%. And for the normal edge crack of length c subject to remotely applied tension σ_a, the equation (17) gave $k_1 = 1.1192\sigma_a\sqrt{\pi c}$ for $n = 50$ ($\Delta l/c = 0.02$) and $k_1 = 1.1231\sigma_a\sqrt{\pi c}$ for $n = 100$ ($\Delta l/c = 0.01$), compared to the exact value $k_1 = 1.1215\sigma_a\sqrt{\pi c}$ of Koiter[8].

In this model of discrete dislocations, there seems to be arbitrariness about how to distribute the dislocations. However, an equal interval provides more accurate results than the other cases. Furthermore, when an equal interval is not permitted as in an infinitesimally kinked crack, a linearly varying interval is adopted so that neighboring segments may have an approximately equal interval. This scheme was found to be an efficient way of distribution when tested upon the normal edge crack.

3. Numerical Examples

3.1 Oblique Edge Crack

The discrete dislocation model is applied to the problem of an oblique edge crack of length c in a semi-infinite plane under uniform tension σ_a, as shown in Fig. 3. Along the crack-line, 60 divisions are made with an equal interval. The Burger's vector normal and parallel to the crack-line at the ith dividing point z_{0i} are respectively

$$b_{i,1} = b_{i,1}(-\sin\alpha, \cos\alpha)$$
$$b_{i,2} = b_{i,2}(\cos\alpha, \sin\alpha) \tag{18}$$

In the equation (13), the stresses in the absence of the crack are constant at all z_j for a given angle α.

$$\sigma_n(z_j) = \sigma_a(1+\cos2\alpha)/2$$
$$\tau_s(z_j) = \sigma_a(\sin2\alpha)/2 \tag{19}$$

The calculated results are shown in Table 1.

Bowie[9] obtained the stress intensity factors for oblique edge cracks in a rectangular panel (panel length/width=2) by a modified mapping collocation method. Thus the crack in the half plane can be approximately compared with the case of the panel width 10 times of the crack length. The maximum difference is that the crack in the panel has about 6% larger value of k_I for $\alpha=0$ and about 7% larger k_{II} for $\alpha=45°$ than those in Table 1. When the finite geometry is taken into account, it is expected that the presented solution has reasonably good accuracy. Note that, for small crack angle of
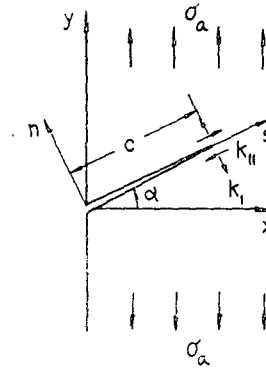

Fig. 3 Oblique edge crack

Table 1 Normalized stress intensity factors for oblique edge cracks under uniform tension. The values in the parenthesis are the mapping collocation solutions[9] for the panel width/ crack length=10

α(degree)	0	10	20	30	40	45	50	60	70
$k_I/\sigma_a\sqrt{\pi c}$	1.123	1.097	1.030	0.924	0.789	0.715	0.641	0.473	0.321
	(1.19)	(1.15)	(1.06)	(0.94)	(0.79)	(0.71)	(0.63)	(0.46)	(0.29)
$k_{II}/\sigma_a\sqrt{\pi c}$	0.000	0.116	0.220	0.300	0.347	0.357	0.354	0.334	0.270
	(0.00)	(0.12)	(0.23)	(0.32)	(0.37)	(0.38)	(0.·38)	(0.34)	(0.27)

order one, the correction factor for the free boundary is $k_1 = 1.12\sigma_n\sqrt{\pi c}$ and $k_{II} = 0.68\tau_s\sqrt{\pi c}$ where σ_n and τ_s are remotely applied stress components given in the equation (19). This result is substantially different from the solution of an angled crack embedded in an infinite plane, especially in the mode II stress intensity.

3.2 Bent Cracks in Half Plane

The configuration of the asymmetric crack is shown in Fig. 4. For the bent crack length $c_i/c > 0.1$, the entire crack-line is divided into 60 segments with an approximately equal interval, in total 120 dislocations. For a crack with a small kink, 50 divisions with linearly varying intervals are taken for the main crack and 10 segments with an equal interval for the pupative kink. In the equation(13), the stresses of the uncracked body are $\sigma_n(z_i) = \sigma_a$ and $\tau_s(z_i) = 0$ for the main crack, and the equation (19)
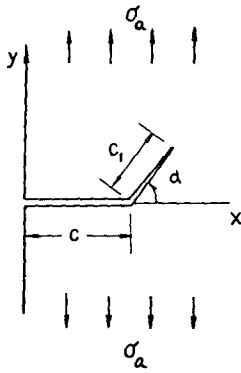
Fig. 4 Bent edge crack

for the bent. Some of the numerical results are presented in Table 2.

In the absence of other available solutions to the author's knowledge, this solution is compared with two approximate expressions suggested for the bent crack in an infinite plane. The stress distributions around a kinked crack with an infinitesimal kink may be approximated with those for the main crack without a kink[2], the SIF of which is denoted with K_1. Thus we get the kinked crack SIF k_1 from the hoop stress σ_θ for the main crack and k_II

Table 2 Normalized stress intensity factors $k_1/(\sigma_a \sqrt{\pi c})$ and $k_\mathrm{II}/\sigma_a \sqrt{\pi c})$ for bent edge cracks under uniform tension

c_1/c	0.01		0.1		0.3		0.5	
Mode	I	II	I	II	I	II	I	II
10°	0.170	0.118	1.177	0.124	1.259	0.134	1.351	0.144
20°	1.127	0.229	1.129	0.240	1.202	0.258	1.287	0.277
30°	1.058	0.328	1.051	0.343	1.113	0.365	1.186	0.390
40°	0.968	0.410	0.950	0.426	0.996	0.448	1.056	0.476
50°	0.862	0.472	0.832	0.485	0.861	0.503	0.906	0.529
60°	0.745	0.512	0.703	0.520	0.717	0.529	0.746	0.547
70°	0.625	0.530	0.570	0.529	0.571	0.525	0.587	0.533
80°	0.506	0.528	0.441	0.513	0.432	0.496	0.439	0.492
90°	0.392	0.508	0.320	0.477	0.306	0.446	0.308	0.429

from the shear stress $\tau_{r\theta}$.

$$k_1/K_1 = \frac{1}{4}\left(3\cos\frac{\alpha}{2} + \cos\frac{3\alpha}{2}\right)$$

$$k_\mathrm{II}/K_1 = \frac{1}{4}\left(\sin\frac{\alpha}{2} + \sin\frac{3\alpha}{2}\right) \qquad (20)$$

where $K_1 = 1.1215 \ \sigma_a \sqrt{\pi c}$ is used for the main crack stress intensity factor of the edge crack. This expression is shown to be accurate to an embedded crack[2]. The mode I SIF k_1 in the equation (20) is in good agreement with the values of $c_1/c = 0.01$ in Table 2. However, like an oblique edge crack, a considerable discrepancy is found in the mode II stress intensity factors. The other approximate scheme proposed by Kitagawa et al[10] for relatively large kinks

is to regard the main crack as a straight extension from the kink, which becomes an angled crack with a crack length of $(c_1 + c/\cos\alpha)$. When this approximation is employed for the bent edge crack, the stress intensity factors are expressed as follows with values $f_1(\alpha)$ and $f_\mathrm{II}(\alpha)$ for oblique edge cracks in Table 1.

$$k_1 = f_1(\alpha) \ \sigma_a \sqrt{\pi(c_1 + c/\cos\alpha)}$$

$$k_\mathrm{II} = f_\mathrm{II}(\alpha) \ \sigma_a \sqrt{\pi(c_1 + c/\cos\alpha)} \qquad (21)$$

This approximation in comparison with the values in Table 2 is good for the bent crack length $c_1/c > 0.1$ since the k_1 values are within 2% up to to the angle $\alpha = 70°$ and the k_II values are within 6% up to $\alpha = 50°$. The difference is further reduced for large c_1/c and small

angle α.

3.3 Symmetrically Branched Edge Cracks

The dislocations in this problem should have a symmetric distribution about $y=0$, as shown in Fig. 5. Along the main crack-line, the non-zero vectors are $\boldsymbol{b}_i = (0, b_i)$. For the branch in $y>0$, the Burger's vectors are the same as in the equation (18), and their corresponding vectors at $\bar{z}_{0i}$ along the lower branch are

$$\boldsymbol{b}_{i,1} = b_{i,1}(\sin\alpha, \ \cos\alpha)$$
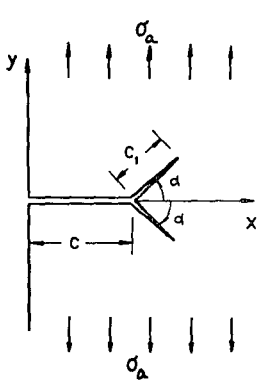$$\boldsymbol{b}_{i,2} = b_{i,2}(-\cos\alpha, \ \sin\alpha) \tag{22}$$

Fig. 5 Symmetrically branched edge crack

The dislocational shear stress along the main crack-line has to be vanished by the symmetry. Thus, in the equation (13), the stresses at z_j due to a dislocation of unit vector on the branches should become, for example,

$$\sigma_{n,1}(z_j, \ z_{0i}) \longrightarrow \sigma_{n,1}(z_j, \ z_{0i})$$
$$+\sigma_{n,1}(z_j, \ \bar{z}_{0i}) \tag{23}$$

Similar superpositions apply to the dislocational stresses. Computations are carried out with 120 dislocations of different magnitudes, and given in Table 3. Even though the lack of available solutions prohibits any direct comparison, it would be interesting to correlate the present solution to an embedded crack with infinitesimal branches. The k_{II} values for $\alpha>30°$ in Table 3 are about 10% larger than the stress intensity factors obtained from finite element calculations[11] and the exact K_I of a normal edge crack. And for the mode I values, there is less than 5% difference between the two solutions for $\alpha=30\sim75°$. In a consequence, the difference between the embedded and edge cracks is small in k_I and large in k_{II} value. That observation is similar to the bent crack with an infinitesimal kink.

Table 3 Normalized stress intensity $k_I/(\sigma_a\sqrt{\pi c})$ and $k_{II}/(\sigma_a\sqrt{\pi c})$ for symmetrically branched edge cracks

c_1/c	0.01		0.1		0.3		0.5	
Mode	I	II	I	II	I	II	I	II
15°	0.714	−0.087	0.723	−0.063	0.868	−0.061	0.955	−0.055
30°	0.794	0.036	0.792	0.074	0.888	0.122	0.957	0.149
45°	0.776	0.182	0.752	0.224	0.804	0.284	0.852	0.318
60°	0.690	0.304	0.643	0.339	0.655	0.391	0.680	0.419
75°	0.558	0.378	0.491	0.397	0.473	0.426	0.478	0.438
90°	0.404	0.397	0.328	0.392	0.290	0.394	0.284	0.386

4. Conclusions

(1) The discrete dislocation method[3] of calculating stress intensity factors for cracks in an infinite plane was extended to the problem of various edge cracks in half plane.

(2) The stress field around an isolated dislocation in a half plane was derived in a compact form of complex functions. And a com-

putational scheme for accurate stress intensity factors from equilibrium Burger's vectors was suggested and tested upon the problems with exact solutions such as normal edge crack in half plane and an angled crack in an infinite plane.

(3) The method was applied to oblique edge cracks, and its results were compared with mapping collocation solutions for similar cracks in a panel with a reasonable agreement. For the bent and symmetrically branched cracks, considerable discrepancy was found between the stress intensity factors of edge and embedded cracks.

References

(1) K.K. Lo, "Analysis of Branched Cracks", ASME J. of Applied Mechanics, Vol. 45, pp. 797~802, 1978

(2) B. Cotterell and J.R. Rice, "Slighty Curved or Kinked Cracks", Int. J. of Fracture, Vol. 16, pp. 155~169, 1980

(3) V. Vitek, "Plane Strain Stress Intensity Factors for Branched Cracks", Int. J. of Fracture, Vol. 13, pp. 481~501, 1977

(4) N.I. Muskhelishvili, Some Basic Problems of the Mathematical Theory of Elasticity, Noordhoff Pub 1953

(5) V. Vitek, "Yielding from a Crack with Finite Root-Radius Loaded in Uniform Tension", J. of Mechanics Physics. of Solids, Vol. 24, pp. 67~76, 1975

(6) J.P. Hirth and J. Lothe, Theoy of Dislocations, 2nd ed., Wiley, New York, 1982

(7) E. Smith, "The Stability of a Wedge Crack under a Uniform Applied Stress", Int. J of Fracture Mechanics, Vol. 1, pp. 204~209, 1965

(8) W.T. Koiter, "Discussion on Rectangular Tensile Sheet with Symmetric Edge Cracks", ASME J. of Applied Mechanics Vol. 32, p. 237, 1965

(9) O.L. Bowie, "Solutions of Plane Crack Prpblems by Mapping Technique", in Methods of Analysis and Solutions of Crack Problems, ed. G.C. Sih, Noordhoff Pub. Leiden, pp. 1~55, 1973

(10) H. Kitagawa, R. Yuuki, and T. Ohira, "Crack-Morphological Aspects in Fracture Mechanics", Engineering Fracture Mechanics, Vol. 7, pp. 515~529, 1975

(11) W.K. Wilson and J. Cherepko, "Analysis of Cracks with Multiple Branches", Int. J. of Fracture, Vol. 22, pp. 303~315, 1983